Beni-Suef University Journal of Basic and Applied Sciences

RESEARCH

Open Access

Flexural performance of rapid-hardening concrete (RHC) beams with tension lap splice

Mohamed Hussein El Fakhrany[1*], Amal el-Zamrawi[1], Wael Ibrahim[1] and Alaa Sherif[1]

Abstract

Background Rapid-hardening concrete (RHC) is a specialized type of concrete that gains strength at an accelerated rate, allowing for faster construction and reduced project timelines. The use of RHC in structural applications, such as in beams subjected to flexural loads, has gained significant attention due to its potential for improving construction efficiency. This study focuses on the flexural performance of RHC beams with tension lap splice, which is considered a common method for joining reinforcement bars in concrete structures.

Results Several parameters were taken into consideration, such as concrete type, concrete cover, and reinforcement bar diameter. The loading test was performed on sixteen beams to show results of load capacities, moment–displacement response, energy absorption, and ductility. As a result, the flexural performance of RHC beams is compared to that of NC beams.

Conclusions Results indicate that RHC beams require 30 Φ splice length after 3 days of casting, while NC beams require 40 Φ splice length after 28 days. The RHC beam had higher load capacities, ductility, resilience, and toughness than NC beams, by 73%, 41%, 82%, and 88%, respectively. The bar diameter and concrete cover had a significant effect on increasing loads and resilience, while toughness decreased.

Keywords Self-compacting, Rapid hardening, Normal strength, Mixes, Workability, Concrete, Temperature, Compressive strength, Mechanical behavior, RHC

1 Background

The rapid-hardening concrete (RHC) is commonly known as concrete with accelerated strength gain and can be used to achieve a fast construction pace [1]. High-performance concrete (HPC) has many requirements, according to ACI [2]. Early-age development, compaction without segregation, toughness, and volume stability are the most important requirements for achieving HPC. Rapid-hardening concrete is a type of high-performance concrete that can be produced using superplasticizers that minimize the water-cement ratio and increase early-age development. Polycarboxylate ether was used to make RHC with high strength and workability. Microsilica is used to block concrete and reduce cracks resulting from the heat hydration process of cement [3–5].

The use of reinforced bar splices in reinforced elements cannot be avoided in several cases. Due to limitation of rebar length, reinforced bars must be connected to construction sites to ensure reinforcement continuity [6]. Lap splicing is the most common method used for splicing reinforced bars [7–11]. A sufficient lap-splice length was used for the transfer of tensile stress between bars through concrete without bond failure [12]. Most previous studies concluded that the lap-splice length has a major effect on the flexural performance of concrete elements. Reynolds et al. [13] concluded that lap-splice performance is affected by the anchorage length. Several parameters were considered in this study, such as concrete strength, concrete cover, and transverse steel, as the main factors in the investigation test. The flexural

*Correspondence:
Mohamed Hussein El Fakhrany
engmohamedhussein04@gmail.com
[1] Department of Civil, Faculty of Engineering, Helwan University, Cairo, Egypt

performance of reinforced concrete beams is directly affected by the overall performance of the structural system. The reinforcement system is a major factor that affects the flexural performance of beams [14]. The code provisions of the ACI [15] and Euro code [16] include many parameters that cannot be considered theoretically. The researchers attempted to use some parameters to determine the accurate splice length.

The demand for RHC with better behavior and lower costs has led to increased research on upgrading or exploiting the structural mechanical performance by introducing innovative materials, structures, and techniques [17–26]. Rui Yu et al. [27] conducted an experiment on rapid-hardening concrete, and their study revealed that the strength developed the fastest at three hours, reaching 55 MPa with a gypsum substitution rate of 15%, which increased to 81 MPa after seven days. Yelbek Utepov et al. [28] tackled the frost resistance challenge in RHC by utilizing micro silica and CaCl2 modifiers, obtaining superior results in freeze–thaw cycles and expanding opportunities in cold climates [29]. Cangino et al. [30] studied the use of rapid-hardening concrete for the construction of a small-span bridge that repairs and reopens within 24 h. Cook et al. [31] studied the flexural performance of reinforced BCSA concrete beams, thus it showed tensile strength and ductility compared to normal concrete. Jacek et al. [32] tested high-early strength concrete that was evaluated for compressive strength without the use of heat. The use of Portland cement can lead to a compressive strength of 36 MPa after 16 h. The flexural behavior of high-strength concrete beams with tension lap splices was investigated by Magda et al. and Azab et al.[33, 34]. The behavior of a tension lap-splice on self-compacting concrete was investigated by Azab et al. [35]. In previous studies, many researchers have investigated RHC mixes, as in the research of Najm et al. [36]. The flexural behavior of RHC beams, which were performed in the research of Wael et al. [37]. The current study aims to investigate the flexural performance of RHC beams with tension lap splices and compare them to normal-strength beams owing to the gap in research in this field.

Researchers have investigated various parameters to understand the flexural behavior and tension-splice strength in concrete [38, 39]. Different design codes specify the minimum required lap-splice length for different bar diameters to prevent splitting. For example, Tepfers et al. [40] concluded that the stress imposed by reinforced bars in concrete can lead to splitting cracks along the longitudinal direction. Hegger et al. [41] reported tests on specimens with two bar sizes reaching bar stresses of up to 600 MPa with lap-splice lengths ranging from 23 to 44 times the bar diameter. Richter et al. [42] tested lap-splices under direct tension in concrete beams. The results showed that, contrary to what is suggested in ACI 408R [43], strength does not increase proportionally with lap-splice length. Glucksman et al. [44] conducted tests of lap splice specimens with high-strength reinforcement and lap splices exceeding 40 (d_p). He found that lap-splice strength is not proportional to its length. Frosch et al. [45]observed that for unconfined lap splices shorter than 80 times the depth, the bar stress increased with the lap length. Micallef et al. [46] investigated the effect of splice length on both ductility and strength by comparing different lap splice lengths. The study indicated that an increase in splice length resulted in improved ductility but decreased lap strength. Wu et al. [47] studied the bond strength of tension lap splices in both self-compacting and conventional concrete beams. Their results showed a similar bond strength behavior between self-compacting and conventional concrete.

The aim of the study was to investigate the performance of RHC beams with tension lap splice under flexural loading and compare it with normal concrete beams. To achieve this, a series of experimental tests are conducted on full-scale RHC beams, along with control specimens made of normal concrete. The specimens are designed and constructed according to relevant design codes and standards.

2 Advances in rapid-hardening concrete

The demand for HPC with high-strength concrete was crucial. Rapid-hardening concrete can achieve a noticeable strength of more than 21 MPa in 24 h while maintaining excellent flexural performance [48]. Concrete's mechanical properties have a significant impact on bond characteristics, making concrete type an important parameter in the study of structural element behavior. Rapid-hardening concrete has distinct microstructures and failure modes during compression compared to normal-strength concrete. The RHC has recently been used in a number of major projects, including the Cairo monorail, which is regarded as one of the most important green transportation systems in the Middle East. The RHC is used to manufacture guideway beams for Cairo monorails, as depicted in Fig. 1. The limited number of molds makes it difficult to pour all of the beams on-site. Although RHC is more expensive than NC, it shortens the project's construction time.

3 Design recommendation for splice length

To calculate the splice length of rapid-hardening concrete beams, a review of code provisions was conducted. International code recommendations by ACI 318R-19 [49], and Egyptian code [50] can be applied to RHC beams.

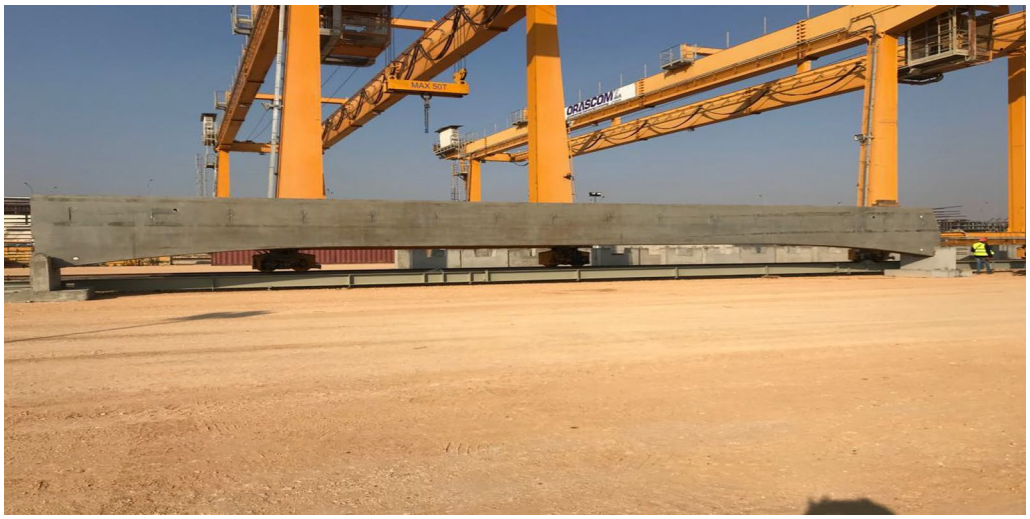

Fig. 1 The monorails guideway beam manufactured from Rapid-Hardening concrete

3.1 ACI 318R-19 [49]

Lap splice not less than larger (300 mm) and (48 d_b) for deformed uncoated bar or wire.

According to ACI [49] Article 25.4.2.4a

$$Ld = \frac{fy}{1.1\lambda\sqrt{fc'}} \frac{\psi t \psi e \psi s \psi g}{(cf + ktr)/dp} \geq 300 \tag{1}$$

$$\begin{aligned} (c_f + k_{tr})/d_p \leq 2.5,\ c_f &= \min(c_b, c_{so}, c_{si}) \\ &\quad + 0.5\, d_p,\ ktr \\ &= 40Atr/sn \end{aligned} \tag{2}$$

Ψ_t is the traditional reinforcement location factor and equal 1 for bottom casted beam. Ψ_e is a coating factor reflecting the effects of epoxy coating = 1. But (Ψ_t X Ψg) not less than 1.7, $\lambda = 1$ for normal weight concrete. Ψ_g is the reinforcement grade and equal 1. Ψ_s is the bar diameter factor and equal 0.8. *fc* is concrete compressive strength and equal 64.3 MPa. *Fy* is steel yielding strength and equal 500 MPa. c_b = thickness of bottom concrete cover. C_{so} = thickness of side concrete cover. C_{si} = one half of the center to center spacing of bars. A_{tr} is the total area of confining reinforcement within spacing across plane. n is the number bars being spliced along the plane. *s* is the center to center spacing of transverse bars. When lap splices are used, the required lap splice is defined as ($1L_d$ or $1.3L_d$).

3.2 Egyptian code (ECP-2020) [50]

$$L_d = [\alpha\beta\eta(f_y/\gamma_s)/(4f_{bu})]\,\Phi \tag{3}$$

According to (ECP-2020) [50], Eq. (3) used to estimate tension splice length for concrete elements. $\eta = 1$ for splices near the bottom surface of beams. B = correction factor for bar surface and equals 0.75 for deformed bars, α = correction factor for bar ends and is equal to 1 for straight bar and 0.75 for the bent and u-shape end, f_{bu} is the bond strength of concrete and equal to $0.3\sqrt{\frac{fc}{\gamma c}}$, f_c is the concrete compressive strength in MPa and γ_c is concrete strength reduction equal 1.5, The compressive strength of RHC and NSC equal 50 MPa, According to ECP-203 [50] clause (4-2-5-4-2-C) the splice length shall be taken = 1.3Ld in case that the actual reinforcement less than double the total required reinforcement area (splice of all reinforcement bars in the same zone).

4 Methods

4.1 Materials properties

The rapid-hardening concrete (RHC) created in the current paper was produced with Portland cement (CEM III 52.5N) from the Suez factory that complied with Egyptian standard specifications. The cement content of RHC and NC is 475 kg/m^3. Clean tap water free from impurities was used for mixing the concrete. Fine aggregates were natural sand with a specific gravity of 2.67 and a fineness modulus of 2.35. Crushed limestone aggregate with a maximum aggregate size of 10 mm the grading of aggregates has been performed to achieve the rheological properties of concrete. The superplasticizers were polycarboxylate ether-based 3rd generation chemical admixtures that allow a reduction of water by 40%. The composition of RHC and NC is presented in

Table 1 Design of the concrete mix (per m^3)

Components (kg/m^3)	Normal concrete	Rapid-hardening concrete
Cem III	475	475
Water	250	174
w/c	0.48	0.35
Coarse aggregate (10mm)	875	875
Fine aggregate (sand)	884	884
superplasticizer HRWR (L/m^3)	–	10
plasticizing agent accelerator (L/m^3)	–	3
Micro silica	25	25

Table 1. It can be noticed that the use of micro silica as a reduction of heat resulted from the cement-hydration process and improved long-term durability. The absolute volume method recommended by ACI [51] was used to determine the required quantities of materials. The RHC mix reaches 63.4 Mpa after 3 days while NC reaches 50 Mpa after 28 days. Reinforcement on the tension side consists of 2 or 3 bars of 10, 12 diameters while two deformed 10 mm in compression zone. Two bar tested form each diameter to express mechanical properties of steel. The mechanical properties of steel are presented in Table 2.

4.2 Rheological properties of RHC

The rheological properties of RHC had been evaluated by several tests of slump-flow and u-test, as shown in Fig. 2. Slump flow was performed according to standard methods defined in Italian standards as illustrated in Fig. 3. The rheological properties of RHC fully satisfy the self-compacting concrete requirement according to Italian standards [52]. To assess the feasibility of using RHC on a construction site where casting operations can take a long time, a test to evaluate slump loss vs. time was conducted. The rheological properties of RHC mixes are depicted in Table 3. The use of polycarboxylate ether in the production of RHC reduces water content while increasing workability.

4.3 Test specimens

The experimental program investigated sixteen simply supported concrete beams reinforced with high-grade steel bars. Each beam contained spliced bars designed to fail in tension within a constant moment zone. The schematic view of the test setup is presented in

Table 2 Mechanical properties of steel

Type	Nom diameter (mm)	Actual diameter (mm)	Yield strength Reh (Mpa)	Tensile strength Rm (Mpa)	Elongation (%) After Breaking	Rm/Reh
High strength Steel grade 500 MPa	10	10.08	589.5	765.9	27	1.30
	12	12.11	587.6	788.9	22.4	1.34
	16	16.13	581.9	729.1	24.3	1.25

Fig. 2 The *U*-test and *L*-Box test

Fig. 2. All specimens had a rectangular cross section of 150 mm × 200 mm, a clear span of 1800 mm, and a total length of 2000 mm, as shown in Fig. 1. The beams were subjected to two concentrated static loads (four-node testing) under simple support conditions. Details of the tested specimens are provided in Table 4 and Fig. 4.

Fig. 3 Slump flow test

Table 3 Rheological properties of RHC and limit values according to UNI 11040 for (SCC)

Test	Test results	Limits value	Notes
Slump flow	D = 750–770 mm	D > 600 mm	D: refer to the diameter of concrete at the end of the test after 90 min = 750
L-box	H_2/H_1 = 1.1	H_2/H_1 > 0.8	H_2, H_1: refer to the height of concrete after and before entering the L—box gate
U-test (T0)	9.8	6–12 s	T: refer to the time of concrete to pass through U-test
U-test (T5)	12.1	T0 + 3s	Second U-test

Table 4 Details of specimens

Group	No	Beam designation	Splice length L_s (mm)	Bar dia. (mm)	Concrete cover (mm)	RFT ratio (ρ)	Type of concrete
I	1	M-L0 × 10-R.852-C20	–	10	20	0.852	RHC
	2	M–L20 × 10-R.852-C20	200 (20Ø)	10	20	0.852	RHC
	3	M–L30 × 10-R.852-C20	300 (30Ø)	10	20	0.852	RHC
	4	M–L40 × 10-R.852-C20	400 (40Ø)	10	20	0.852	RHC
II	5	M–L0 × 12-R.852-C20	–	12	20	0.852	RHC
	6	M–L20 × 12-R.852-C20	240 (20Ø)	12	20	0.852	RHC
	7	M–L30 × 12-R.852-C20	360 (30Ø)	12	20	0.852	RHC
	8	M–L40 × 12-R.852-C20	480 (40Ø)	12	20	0.852	RHC
III	9	M–L0 × 10-R.902-C30	–	10	30	0.902	RHC
	10	M–L20 × 10-R.902-C30	200 (20Ø)	10	30	0.902	RHC
	11	M–L30 × 10-R.902-C30	300 (30Ø)	10	30	0.902	RHC
	12	M–L40 × 10-R.902-C30	400 (40Ø)	10	30	0.902	RHC
IV	13	N–L0 × 10-R.852-C20	–	10	20	0.852	NC
	14	N–L20 × 10-R.852-C20	200 (20Ø)	10	20	0.852	NC
	15	N–L30 × 10-R.852-C20	300 (30Ø)	10	20	0.852	NC
	16	N–L40 × 10-R.852-C20	400 (40Ø)	10	20	0.852	NC

RHC beams tested at age 3 days while NC beams tested at 28 days

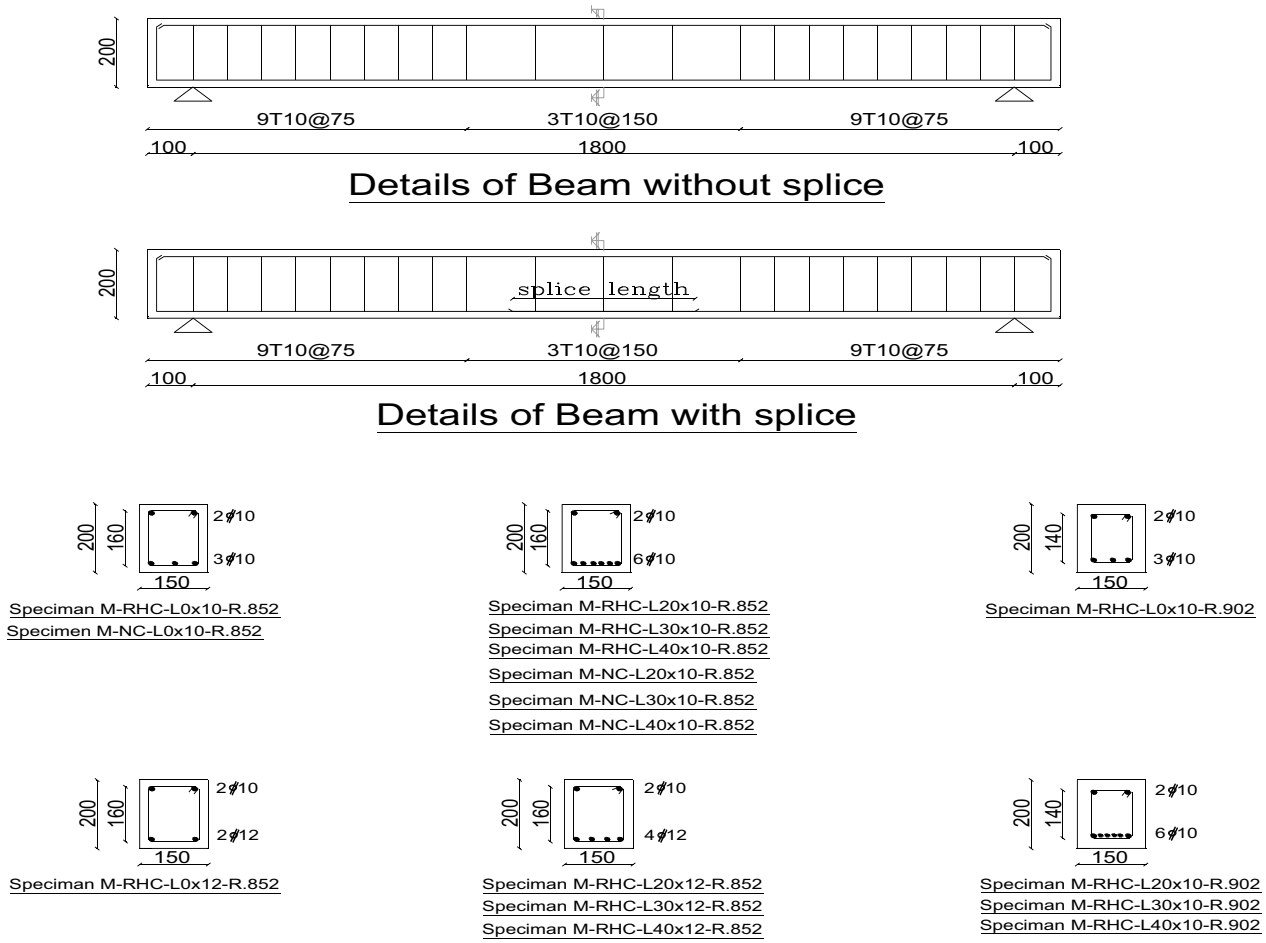

Fig. 4 Reinforcement details and concrete dimensions for all Beams

A four-part notation system is used to identify the variables for each specimen:

Part 1: Concrete type ("M" for rapid-hardening concrete, "N" for normal concrete).
Part 2: Splice length as a factor of bar diameter (e.g., "L20" for 20 times bar diameter).
Part 3: Reinforcement ratio ("R0.852", "R0.902" for 0.852 and 0.902 reinforcement ratio, respectively).
Part 4: Concrete cover ("C20", "C30" for 20 mm and 30 mm cover, respectively).

Unspliced specimens are designated as "control specimens."

The beams were designed according to the Egyptian code of practice.

Group (A): consists of four beams with the same reinforcement ratio of 0.852% and concrete cover of 20 mm but different in splice length (0, 20, 30 and 40) times bar diameter 10 mm. **Group (B)**: consists of four beams with the same reinforcement ratio of 0.852% and concrete cover 20 mm but different in splice length (0, 20, 30 and 40) times bar diameter 12 mm.

Group (C): consists of four beams with the same reinforcement ratio 0.852% and concrete cover 30 mm but different in splice length (0, 20, 30 and 40) times bar diameter 10 mm.

Group (D): consists of four beams with the same reinforcement ratio of 0.852% and concrete cover 20 mm but different in splice length (0, 20, 30 and 40) times bar diameter 10 mm. The main difference from group (A) is the concrete type (normal concrete).

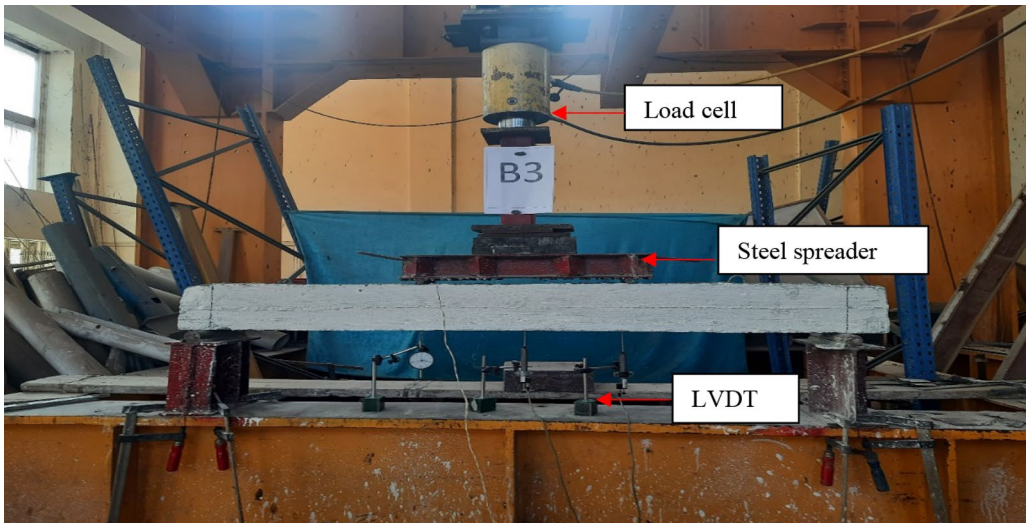

Fig. 5 A photograph of the test setup

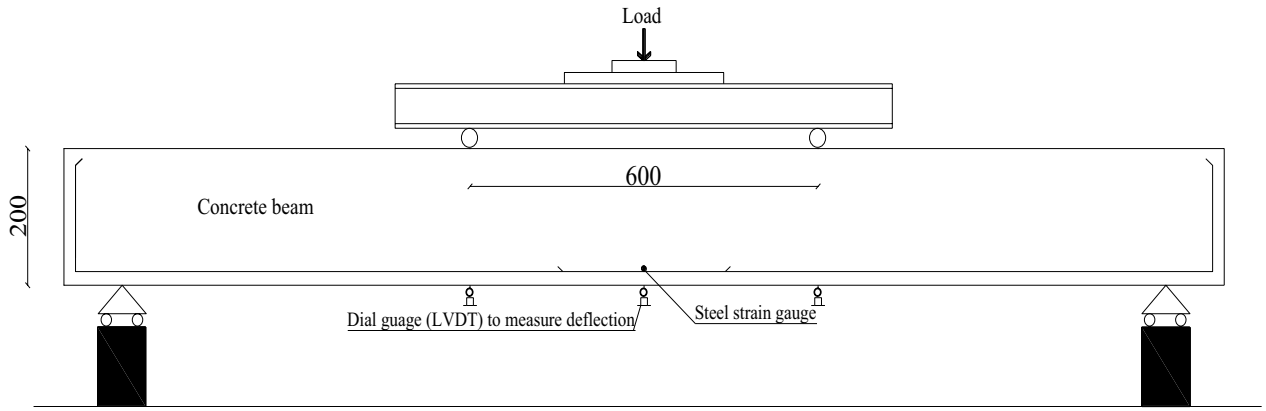

Fig. 6 The schematic view of the test setup (dimension in mm)

4.4 Test procedure

A static hydraulic loading jack equipped with an electrical load cell applied the vertical load. A digital indicator with 1 kN accuracy measured the applied load. Each beam was centered in the testing machine as shown in Fig. 5. A schematic view of the test setup is illustrated in Fig. 6. Loads were applied in increments of 2.5 kN. At each increment, cracks were observed, marked, and readings were taken for deflection and steel strain. Failure was determined as the point where the load could no longer increase. Deflection at mid-span and under concentrated loads was measured using a dial gauge with 0.01 mm accuracy via LVDT. Crack propagation on the concrete beams was plotted during loading. Steel strain at mid-span was measured using a 60-mm gauge length on one deformed bar within the splice region.

5 Results

5.1 Compressive and tensile strength

The compressive and tensile strengths of the concrete samples were evaluated in accordance with the EN 12390-2:2009 testing protocol [53]. An automated hydraulic press was employed for both compression and tension tests. For each concrete age, three cubes and cylinders were fabricated from the same concrete mix as the tested specimens. Compressive strength was calculated using the applied failure load divided by the cube cross-sectional area ($f_c = f/A_c$). The tensile strength

Table 5 Compressive and Tensile strength of the concrete mix

Concrete mix	Ages	Compressive strength (MPa)	Tensile strength (MPa)
RHC	8 h	31.0	3.0
	16 h	39.0	4.2
	24 h	44.5	5.8
	3D	63.4	8.9
	7D	70.0	10.1
	28D	81.2	11.1
	56D	85.1	11.6
	90D	90.0	11.9
NC	24 h	10.0	2.3
	3D	20.0	4.0
	7D	31.8	4.7
	28D	50.0	5.6
	56D	53.1	5.8
	90D	55.2	6.0

calculation utilized the applied failure load, cylinder diameter (d), and cylinder length (L), following the formula $f_{ct} = 2f/\Pi.L.d$. Table 5 summarizes the compressive and tensile strength results obtained at 8, 16, 24 h, and 7 and 28 days. Figure 7 illustrates the failure modes observed in the tested cubes and cylinders. Figures 8 and 9 visually represent the compressive and tensile properties of both RHC and NC concrete mixes.

5.2 Failure modes and load capacities

The experimental results for all specimens are presented in Table 6. The flexural capacity of the specimen reinforced with 10 mm was higher than that of the specimen reinforced with 12 mm. The flexural capacity of the specimen with a concrete cover of 20 mm was higher than that of the specimen with a concrete cover of 30 mm. The flexural capacity of rapid-hardening concrete is higher than that of normal concrete. The flexural capacities of the specimens are presented in Table 6. A comparison of the flexural capacities of the groups is shown in Fig. 10. The crack growth and failure of all the beams are shown in Figs. 11, 12, 13 and 14. Each beam started to crack at approximately the same load and flexural stiffness as the other beams did. It can easily be observed that the crack initiated from the splice ends at a constant moment zone, and failure occurred after a longitudinal crack occurred in the splice region along the tensile reinforcement at the edge of the splice and extended to the mid-span. All beams reached their capacity by flexural failure. Only four specimens failed owing to slippage. The remaining beams failed in a flexural manner. All specimens with a splice length of 20 Ø failed by slippage as they failed to transfer stress along the splice length. The crack load of the specimen reinforced with 12 mm steel was higher than that of the specimen reinforced with 10 mm steel. The crack load of the specimen with a concrete cover of 30 mm was higher than that of specimen with a concrete cover of 20 mm. The crack load of rapid-hardening concrete is higher than that of normal concrete, owing to its higher strength development. The ultimate load of the specimen reinforced with 10 mm was higher than that of the specimen reinforced with 12 mm, except for that of the control specimen without a splice. The ultimate load of the specimen with a concrete cover of 30 mm was higher than that of specimen with a concrete cover of 20 mm, except for the control specimen. The ultimate load of RHC is higher than that of normal concrete. The

Fig. 7 Mode of failure of specimens

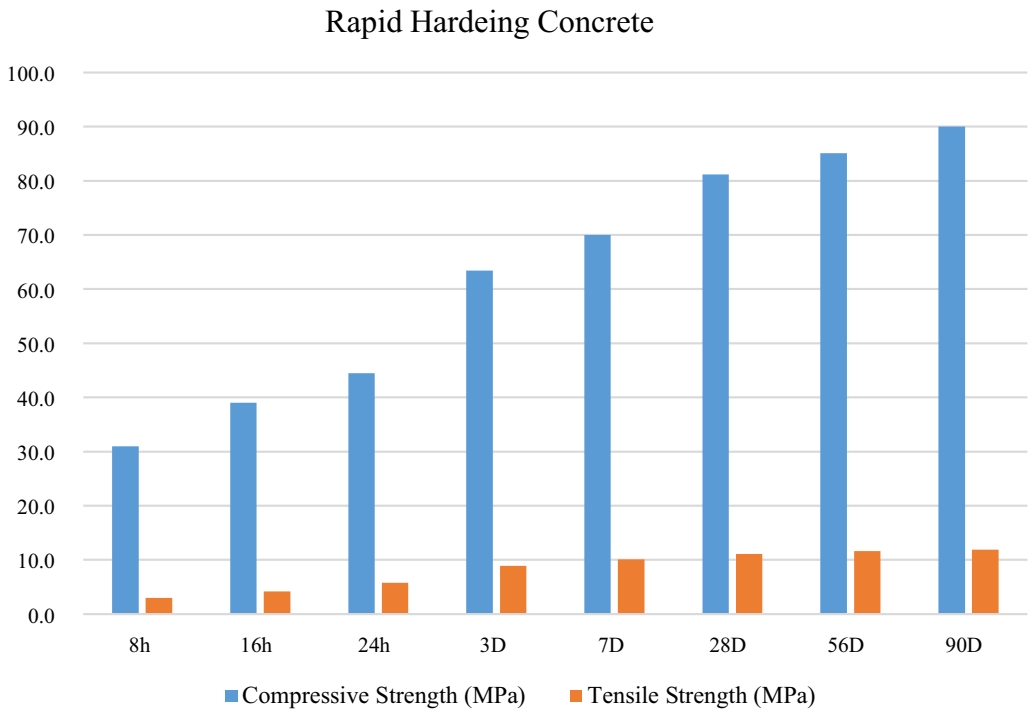

Fig. 8 The compressive and tensile strength for RHC

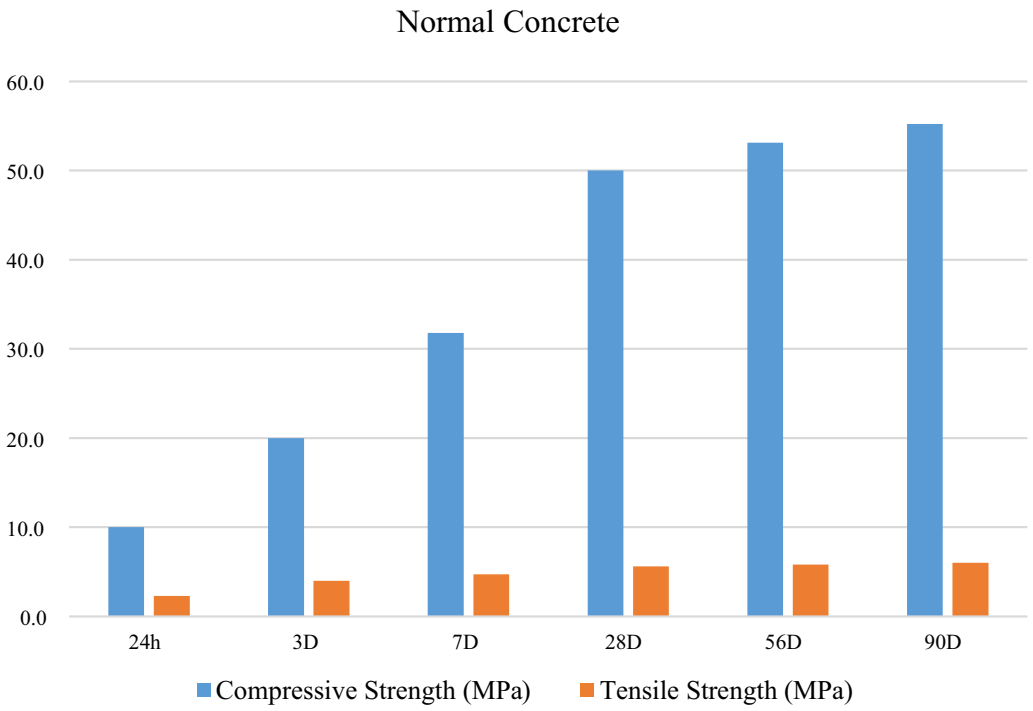

Fig. 9 The compressive and tensile strength for NC

Table 6 Experimental results

Group	Beam ID	Pcr	Δ cr	Mcr	Pu	Δu	Mu	Δy	μ	T	R	Failure mode
I	M-L0×10-R.852-C20	21.3	2.0	12.8	93.8	32.6	56.3	10.6	3.1	33.8×10^2	3.3×10^2	Flexure
	M-L20×10-R.852-C20	20.0	1.5	12.0	117.5	19.5	70.5	11.3	1.7	27.5×10^2	4.8×10^2	Slippage
	M-L30×10-R.852-C20	33.8	2.7	20.3	110.0	54.5	66.0	11.9	4.6	38.8×10^2	5×10^2	Flexure
	M-L40×10-R.852-C20	47.5	3.2	28.5	120.0	33.8	72.0	7.8	4.4	45.6×10^2	3.1×10^2	Flexure
II	M-L0×12-R.852-C20	37.5	3.4	22.5	98.8	25.0	59.3	10.3	2.4	35×10^2	3.8×10^2	Flexure
	M-L20×12-R.852-C20	35.0	3.3	21.0	85.0	17.0	51.0	9.1	1.9	32.5×10^2	2.5×10^2	Slippage
	M-L30×12-R.852-C20	56.3	7.9	33.8	103.8	32.0	62.3	13.1	2.4	51.3×10^2	5×10^2	Flexure
	M-L40×12-R.852-C20	33.8	1.8	20.3	108.8	27.8	65.3	7.9	3.5	45.8×10^2	2.9×10^2	Flexure
III	M-L0×10-R.902-C30	35.0	2.9	21.0	87.5	10.5	52.5	8.1	1.3	16×10^2	2.3×10^2	Flexure
	M-L20×10-R.902-C30	61.3	4.3	36.8	146.3	19.9	87.8	11.9	1.7	31.9×10^2	6.9×10^2	Slippage
	M-L30×10-R.902-C30	36.3	2.4	21.8	136.3	18.5	81.8	10.3	1.8	18.1×10^2	5.6×10^2	Flexure
	M-L40×10-R.902-C30	47.5	3.0	28.5	150.0	28.0	90.0	12.5	2.2	33.8×10^2	7.4×10^2	Flexure
IV	N-L0×10-R.852-C20	13.8	1.9	8.3	75.9	37.2	45.5	12.4	3.0	30.3×10^2	3×10^2	Flexure
	N-L20×10-R.852-C20	25.3	3.1	15.2	44.9	7.2	26.9	5.8	1.3	8.1×10^2	1.2×10^2	Slippage
	N-L30×10-R.852-C20	17.3	2.5	10.4	59.8	10.6	35.9	9.2	1.2	8.4×10^2	2.1×10^2	Flexure
	N-L40×10-R.852-C20	19.6	3.0	11.7	74.8	39.7	44.9	9.2	4.3	33.4×10^2	2.3×10^2	Flexure

Pcr: crack load (kN)

Pu: ultimate load (kN)

Δcr: deflection at crack load (mm)

Δ*u*: deflection at ultimate load (mm)

Δ*y*: deflection at yield load (mm)

Mcr: crack moment (kN m)

Mu: ultimate moment (kN m)

μ: ductility index = Δ*u*/Δy

T: toughness (kN mm)

R: Resilience (kN mm)

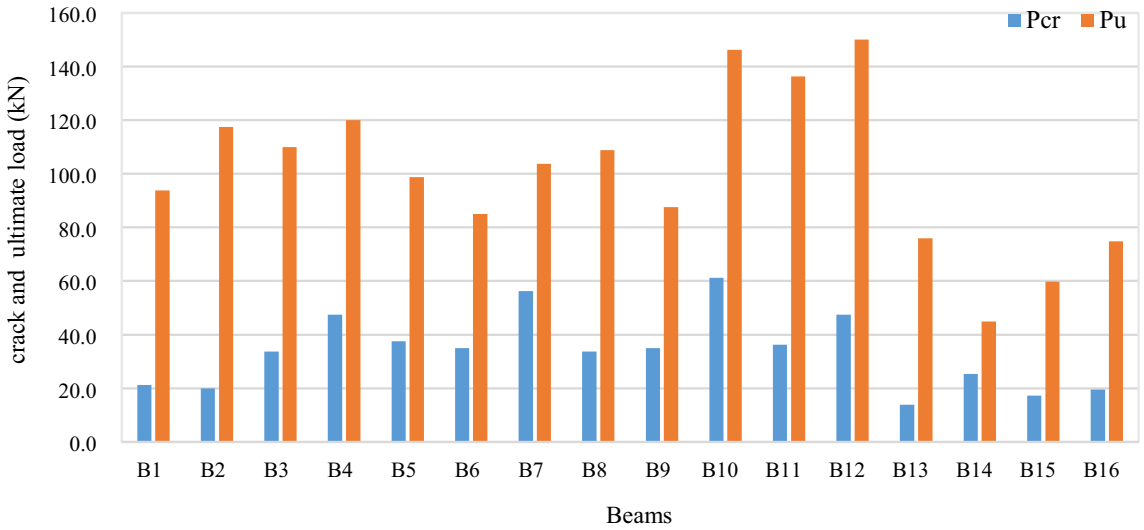

Fig. 10 The crack and ultimate load for all beams

Fig. 11 The crack pattern for group (I)

minimum splice for RHC beams is 30Ø, while for NC beams is 40Ø.

5.3 The moment–displacement response

The moment–displacement response curves of all specimens are shown in Fig. 15. The moment–displacement curves of all beams can be divided into two zones. In the first zone, the moment–displacement curves of all specimens are linear with increasing load until it reached yield point. In the second zone, the curves lose their linearity starting from the yield point until it reached failure.

5.4 Displacement ductility

Ductility is defined as the ability to withstand non-elastic behavior. The ductility of a structural element is proportional to the amount of energy gained under a given load. The ductility index is used to assess the ductility of structural elements [54]. The ductility factor (μ) is the ratio of a structural element's displacement at the ultimate zone (Δu) to its displacement at the yield zone (Δy) [55], as illustrated in Fig. 16. The displacement corresponding to the maximum load (Δu) is easily calculated. To calculate displacement (Δy), draw two tangents on the end yielding and find the maximum point of the load–deflection curve at the intersection point. The ductility index for all samples is shown in Fig. 17. The effect of bar diameter on ductility can be easily observed. By increasing the bar diameter from 10 to 12 mm, the average ductility of the specimen decreases. The effect of concrete cover on the ductility by increasing cover from 20 to 30 mm, the average ductility of the specimen decreases. The ductility of a rapid-hardening concrete specimen is higher than normal concrete specimen except for the control beam without a splice.

Fig. 12 The crack pattern for group (II)

5.5 Resilience

The area under the elastic zone until the yield point can be defined as resilience. The resilience of all beams is shown in Fig. 18. The ability of the structural elements to deform elasticity can be defined by the yield point of the elastic zone. The resilience of the specimen reinforced with a bar diameter of 10 mm was higher than that of the specimen reinforced with a bar diameter of 12 mm. The resilience of the specimen with a concrete cover of 20 mm was less than that of the specimen with a concrete cover of 30 mm. The resilience of rapid-hardening concrete was higher than that of normal concrete, except for the control specimen without a splice.

5.6 Toughness

Toughness is the capability of a material to absorb energy and deform plasticity without any fracture. It considers the properties of a material that can be analyzed in terms of the critical stress intensity. The energy absorption was very close to the definition of toughness. Energy absorption is an important property of structural elements. The energy absorption is directly proportional to the area under the load–deflection curve. The total area under the curve was calculated by adding the two successive displacement zones. The toughness of all samples is shown in Fig. 19. Increasing the bar diameter from 10 to 12 mm increased the toughness of the specimen. The specimen gains more load to

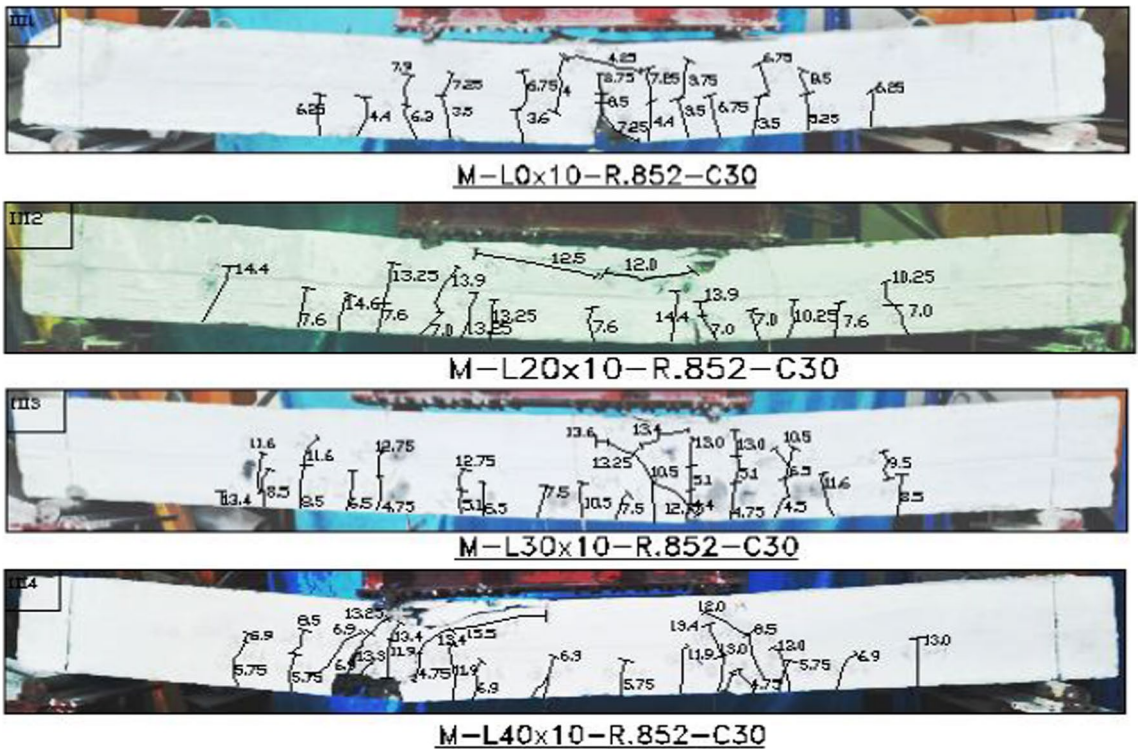

Fig. 13 The crack pattern for group (III)

reach the failure point. When the concrete cover was increased from 20 to 30 mm, the toughness of the specimen decreased. The toughness of the rapid-hardening concrete specimens was higher than that of the normal concrete specimens, except for the control specimens without a splice.

6 Discussion

6.1 Effect of splice length on the flexural performance

The effect of the splice length on the general behavior of the beams depends on several parameters tested experimentally in this study. All specimens failed flexurally, except for four that failed in slippage. The specimen with a splice length of 20Ø failed to slip because it failed to transfer stress along the splice length. The first crack occurred at 30% of the ultimate load of the RHC beams and 20% of the ultimate load of the NC beam. The specimen with a splice length of 20 Ø exhibited a 25.2% and 45.5% higher ultimate load and resilience, respectively, compared to the control specimen without a splice. The crack load, ductility, and toughness decreased by 6.1%, 45.2%, and 18.6%, respectively. The specimens with splices of 30 and 40 Ø exhibited higher crack load, ultimate load, ductility, resilience, and toughness than the control specimen by averages of 90.8%, 22.6%, 45.2%, 23%, and 22.7%, respectively. Previous studies performed by Magda et al. [33] and Azab et al. [34, 35] concluded that the minimum required splice length is 40Ø in high-strength concrete and self-compacting concrete. The minimum splice length required in this paper was 30Ø for the RHC. Moreover, the splice length of 40Ø shows the best performance for rapid-hardening concrete and normal concrete beams. Safe design of splice length in RHC beams is based on the required splice-length design recommendations from different codes. Based on the results of the experimental study and code provisions, the lap-splice length required to satisfy the yielding of the reinforced bars and load capacity exceeding the control specimens is presented in Table 7.

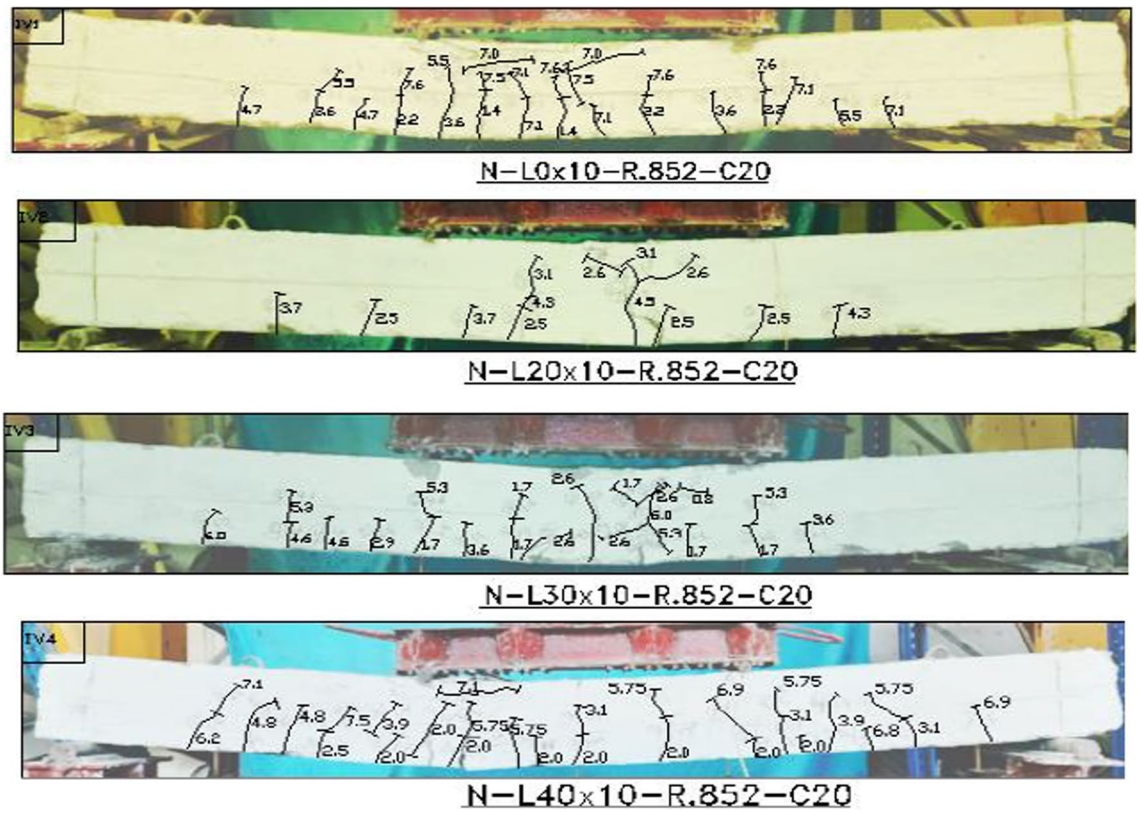

Fig. 14 The crack pattern for group (IV)

6.2 Effect of bar diameter on the flexural performance

The effect of bar diameter on the reinforcement of the beams had a positive effect on the splice zone of the beam (maximum positive moment). The beams reinforced with 10 mm exhibited an average ultimate load, ductility, and resilience of 11.3%, 35.3%, and 14.1%, respectively. Crack load and toughness reduced by an average of 24.6%, 11.5 %, respectively. These results agree with those of Azab et al. [35], who concluded that using a smaller bar diameter with the same reinforcement ratio increases the beam ductility and capacity.

6.3 Effect of concrete cover on the flexural performance

The side and bottom concrete covers had a major effect on determining the suitable splice length. By increasing the concrete cover from 20 to 30 mm, the resilience, crack, and ultimate load increased by an average of 37%, 47%, and 18%, respectively. The ductility and toughness of the beam with a concrete cover of 20 mm were higher than those of the beam with a concrete cover of 30 mm by averages of 97% and 46%, respectively. Magda et al. [33] concluded that increasing concrete cover reduces cracks and ultimate loads, as well as stiffness and ductility of beams. However, this does not agree with the results of the present study. The effect of various concrete covers on utilizing the splice-length value.

6.4 Effect of concrete type on the flexural performance

The compressive strength of concrete varies depending on its type. RHC compressive strength was 27% higher than that of NC after 28 days. The RHC beam outperformed the NC beams in terms of load capacity, ductility, resilience, and toughness by 73%, 41%, 82%, and 88%, respectively. The first crack occurred at 30% of the ultimate load of the RHC beam and 20% of the ultimate load in the NC beams.

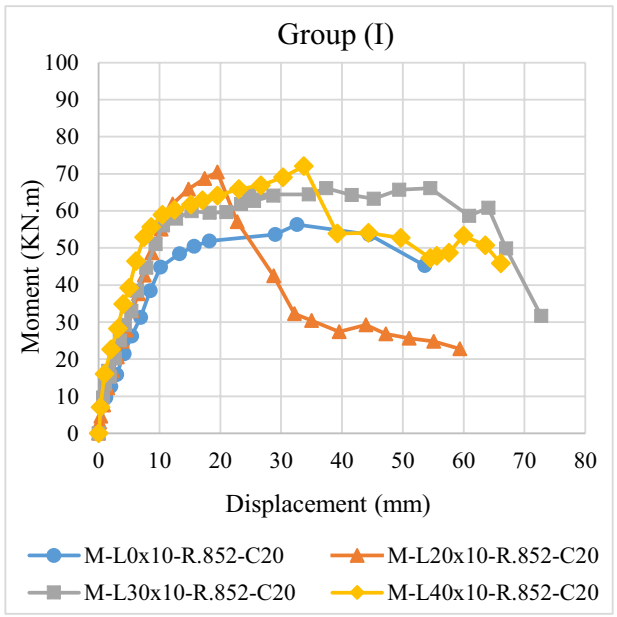

Moment-displacement curve for a group (I)

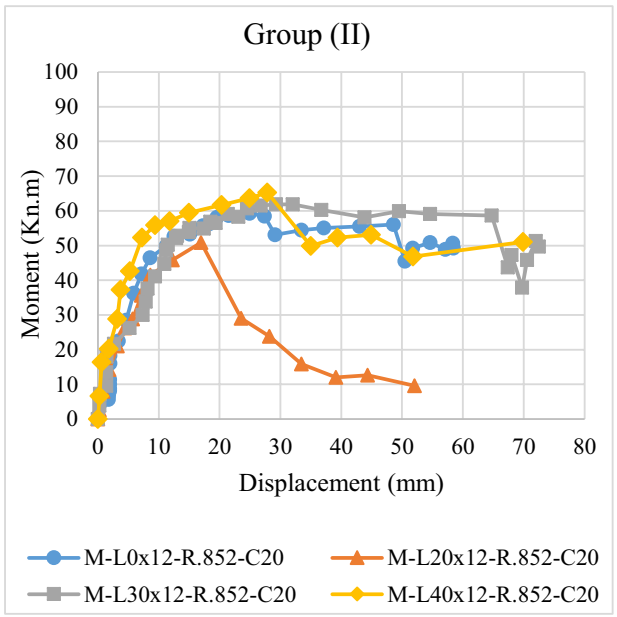

Moment-displacement curve for group (II)

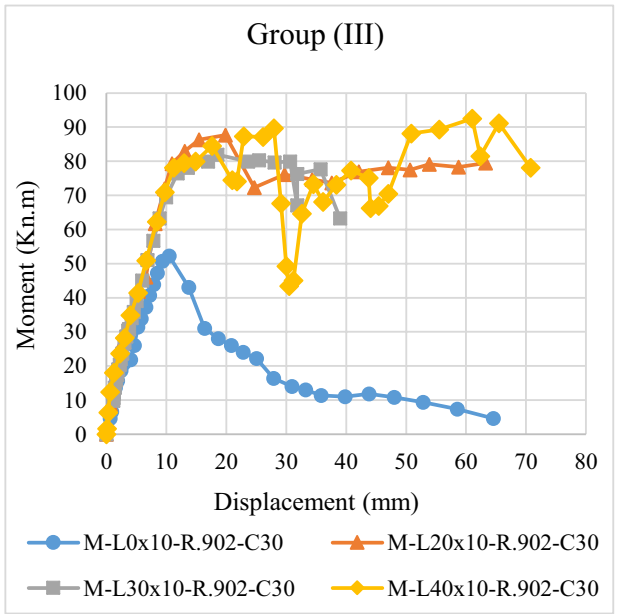

Moment-displacement curve for a group (III)

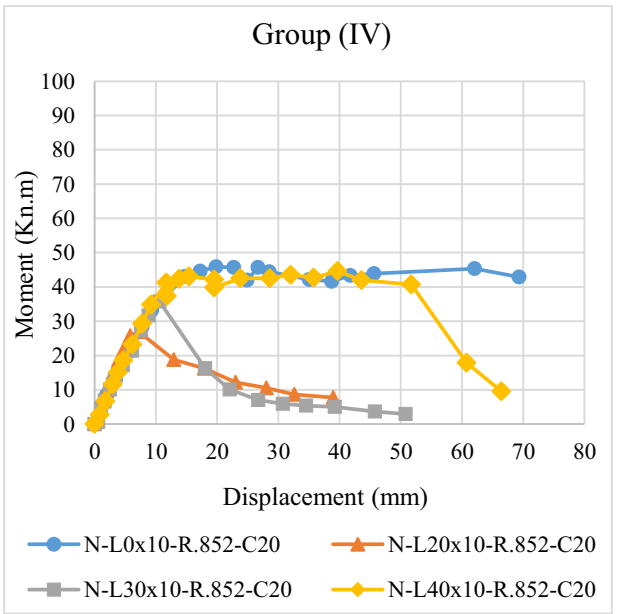

Moment-displacement curve for group (IV)

Fig. 15 Moment–displacement curve for all specimen

7 Conclusion

In this study, the flexural performances of rapid-hardening concrete and normal concrete beams with a tension lap splice were compared. All specimens were compared in terms of load capacity, moment displacement, ductility, resilience, toughness, and failure mechanism. The results are summarized as follows.

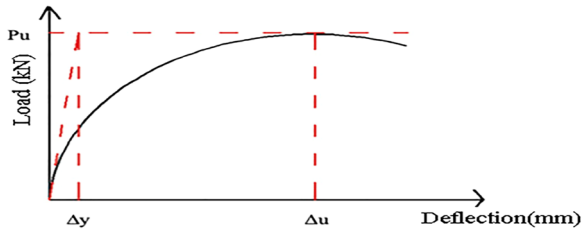

Fig. 16 The displacement ductility ratio definition

The results indicate that RHC beams require a splice length of 30 Φ after three days of casting, while NC beams require a splice length of 40 Φ after 28 days. Increasing the bar diameter from 10 to 12 mm resulted in higher ultimate load, ductility, and resilience by an average of 11%, 35%, and 14%, respectively. The change in the concrete cover from 20 mm to 30 the load capacities and resilience by an average of 18% and 37, respectively.

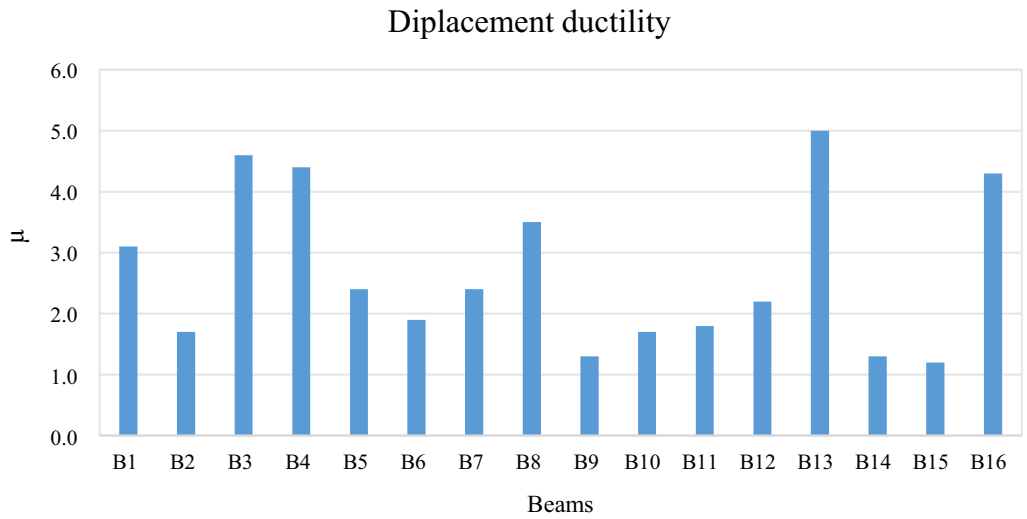

Fig. 17 The displacement ductility of all beams

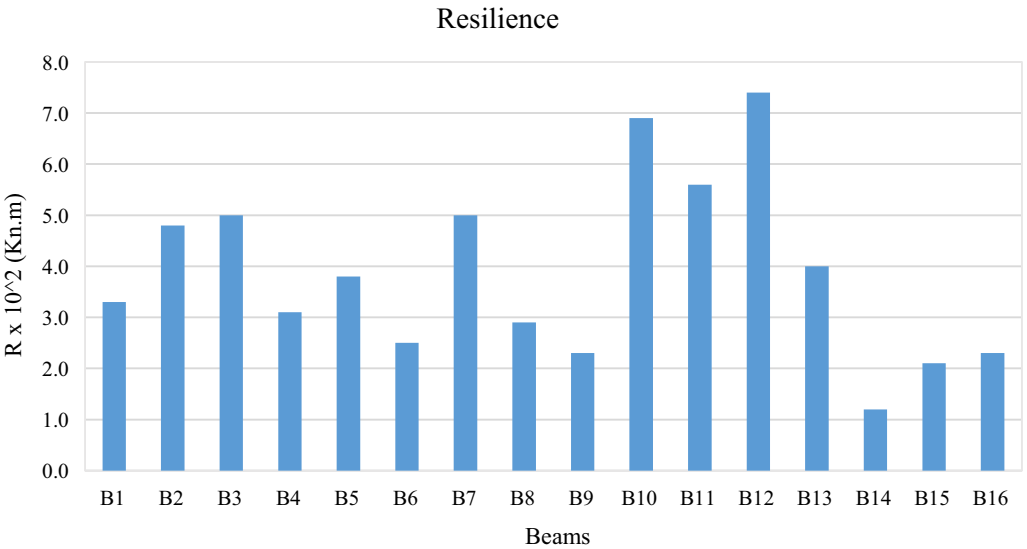

Fig. 18 The resilience of all beams

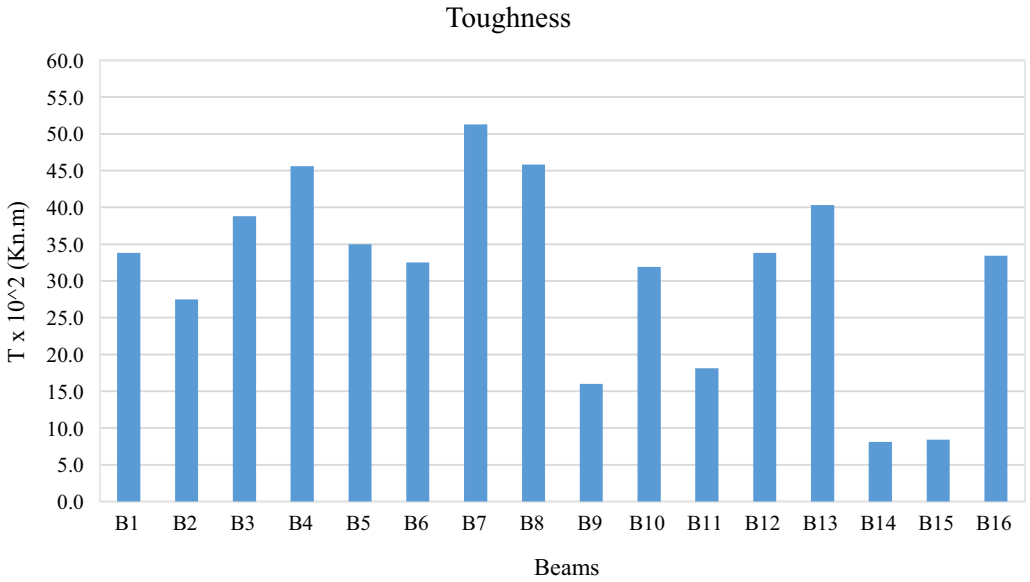

Fig. 19 The toughness of all beams

Table 7 Required lap splice length of tested beams

Group	Beam designation	$L_{d,\ ECP}$	$L_{d,\ ACI}$	$L_{d,\ specimen}$
I	M–L20×10-R.852-C20	418	300	200
	M–L30×10-R.852-C20	418	300	300
	M–L40×10-R.852-C20	408	300	400
II	M–L20×12-R.852-C20	502	300	240
	M–L30×12-R.852-C20	502	300	360
	M–L40×12-R.852-C20	502	300	480
IV	M–L20×10-R.902-C30	418	300	200
	M–L30×10-R.902-C30	418	300	300
	M–L40×10-R.902-C30	418	300	400
VII	N–L20×10-R0.852-C20	408	321	200
	N–L30×10-R0.852-C20	408	321	300
	N–L40×10-R0.852-C20	408	321	400

The ductility and toughness were reduced by 49% and 31%. The concrete type had a significant effect on the flexural performance of the beams. The RHC beams had higher loads, ductility, resilience, and toughness than the NC beams by 73%, 41%, 82%, and 88%, respectively. They recommended the use of a new type of admixture in the manufacture of rapid-hardening concrete. Furthermore, significant research efforts are required to bridge the knowledge gap in this field and facilitate the practical application of this technology to diverse concrete elements such as slabs and columns.

Abbreviations

RHC Rapid-hardening concrete
NC Normal concrete
SCC Self-compacting concrete

Acknowledgements
Authors acknowledge all the staff and technician at Helwan University—Mataria Branch—specially at concrete and material laboratory.

Author contributions
All authors contributed to study the conception and design. Material preparation, data collection, experimental tests and analysis were performed by corresponding author and then approved and revised by other authors. All authors read and approved the final manuscript.

Funding
Authors declare that no funds, grants or other supports was received during the preparation of manuscript. The authors have no relevant finance or non-financial to disclose.

Availability of data and materials
All data are available.

Declarations

Ethics approval and consent to participate
No ethics approval was required.

Consent for publication
Applicable because the manuscript does not contain individual personal data.

Competing intersects
Authors declare no competing intersect.

Received: 17 July 2023 Accepted: 27 February 2024
Published online: 12 March 2024

References

1. Park J-S, Kim YJ, Cho J-R, Jeon S-J (2015) Early-age strength of ultra-high performance concrete in various curing conditions. Materials 8:5537–5553. https://doi.org/10.3390/ma8085261
2. Standard AA (2011) Building code requirements for structural concrete (ACI 318-11). American Concrete Institute
3. Janowska-Renkas E (2015) The influence of the chemical structure of polycarboxylic superplasticizers on their effectiveness in cement pastes. Procedia Eng 108:575–583
4. Neville AM (1995)Properties of concrete, vol 4. Longman, London
5. Perfilov VA, Oreshkin DV, Zemlyanushnov DY (2016) Concrete strength and crack resistance control. Procedia Eng 150:1474–1478
6. Dar ZA, Ashish E (2022) The behaviour of reinforced concrete beams with lap splices using headed bars, 138–145
7. Irheem MM, El-Nawawy OA, Gheith HH (2018) Behavior of RC beams with tension lap splices exposed to fire: experimental study. Int J Civil Eng Technol 9:9–17
8. Leroy A. Lutz and Narendra K. Gosain SAM. Changes to and applications of development and lap splice length provisions for bars in tension (ACI 318–89). ACI Struct J n.d.;90. https://doi.org/10.14359/3980
9. Rezansoff T, Akanni A, Sparling B (1993) Tensile lap splices under static loading: a review of the proposed ACI 318 code provisions. Struct J 90:374–384
10. Azizinamini A, Pavel R, Hatfield E, Ghosh SK (1999) Behavior of lap-spliced reinforcing bars embedded in high-strength concrete. Struct J 96:826–835
11. Esfahani MR, Rangan BV (1998) Bond between normal strength and high-strength concrete (HSC) and reinforcing bars in splices in beams, vol. 95
12. EL-Hawary MM, Kassem AT, EL-Nady AM (2013) Flexural behavior of rectangular concrete beams with lap splices between deformed and smooth reinforcement bars. Int J Eng Res Technol 2:956–962
13. Reynolds GC (1982) Bond strength of deformed bars in tension
14. Gulec A, Kose MM, Gogus MT (2021) Experimental investigation of flexural performance of T-section prefabricated cage reinforced beams with self-compacting concrete. Structures 33:2190–2197. https://doi.org/10.1016/j.istruc.2021.05.074
15. Committee A (2019) ACI 318-19: Building code requirements for structural concrete and commentary. American Concrete Institute: Farmington Hills, MI, USA
16. Arya C (2015) Eurocode 2: design of concrete structures, vol 3. https://doi.org/10.1201/b18121-18
17. Al-musawi H, Huang H, Di Benedetti M, Guadagnini M, Pilakoutas K (2022) Effect of shrinkage on rapid hardening plain and recycled steel fibre concrete overlays. Cem Concrete Compos 125:104246. https://doi.org/10.1016/j.cemconcomp.2021.104246
18. Zhao B, Liu C, Wu H, Ge Y, Yang J, Yi Q (2019) Study on out-of-plane flexural stiffness of unstiffened multi-planar CHS X-joints. Eng Struct 188:137–146. https://doi.org/10.1016/j.engstruct.2019.03.023
19. Xiong Z, Lin L, Qiao S, Li L, Li Y, He S et al (2022) Axial performance of seawater sea-sand concrete columns reinforced with basalt fibre-reinforced polymer bars under concentric compressive load. J Build Eng 47:103828. https://doi.org/10.1016/j.jobe.2021.103828
20. Sun J, Lin S, Zhang G, Sun Y, Zhang J, Chen C et al (2021) The effect of graphite and slag on electrical and mechanical properties of electrically conductive cementitious composites. Constr Build Mater 281:122606. https://doi.org/10.1016/j.conbuildmat.2021.122606
21. Zhao BD, Chen Y, Liu CQ, Wu HD, Wang T, Wei XD (2019) An axial semi-rigid connection model for cross-type transverse branch plate-to-CHS joints. Eng Struct 181:413–426. https://doi.org/10.1016/j.engstruct.2018.12.042
22. Feng W, Tang Y, He W, Wei W, Yang Y (2022) Mode I dynamic fracture toughness of rubberised concrete using a drop hammer device and split Hopkinson pressure bar. J Build Eng 48:103995. https://doi.org/10.1016/j.jobe.2022.103995
23. Cao X-Y, Feng D-C, Beer M (2023) Consistent seismic hazard and fragility analysis considering combined capacity-demand uncertainties via probability density evolution method. Struct Saf 103:102330. https://doi.org/10.1016/j.strusafe.2023.102330
24. Fang S, Li L, Luo Z, Fang Z, Huang D, Liu F et al (2023) Novel FRP interlocking multi-spiral reinforced-seawater sea-sand concrete square columns with longitudinal hybrid FRP–steel bars: monotonic and cyclic axial compressive behaviours. Compos Struct 305:116487. https://doi.org/10.1016/j.compstruct.2022.116487
25. Bida Z, Ke K, Chengqing L, Li H (2020) Computational model for the flexural capacity and stiffness of eccentric RHS X-connections under brace out-of-plane bending moment. J Struct Eng 146:4019227. https://doi.org/10.1061/(ASCE)ST.1943-541X.0002507
26. Cao X-Y, Feng D-C, Wang C-L, Shen D, Wu G (2023) A stochastic CSM-based displacement-oriented design strategy for the novel precast SRC-UHPC composite braced-frame in the externally attached seismic retrofitting. Compos Struct 321:117308. https://doi.org/10.1016/j.compstruct.2023.117308
27. Yu R, Zhang X, Hu Y, Li J, Zhou F, Liu K et al (2022) Development of a rapid hardening ultra-high performance concrete (R-UHPC): from macro properties to micro structure. Constr Build Mater 329:127188. https://doi.org/10.1016/j.conbuildmat.2022.127188
28. Abdraimov I, Kopzhassarov B, Kolesnikova I, Akhmetov DA, Madiyarova I, Utepov Y (2023) Frost-resistant rapid hardening concretes. Materials 16:3191
29. Ghanei A, Eskandari-Naddaf H, Ozbakkaloglu T, Davoodi A (2020) Electrochemical and statistical analyses of the combined effect of air-entraining admixture and micro-silica on corrosion of reinforced concrete. Constr Build Mater 262:120768
30. Cangiano S, Meda A, Plizzari GA (2009) Rapid hardening concrete for the construction of a small span bridge. Constr Build Mater 23:1329–1337. https://doi.org/10.1016/j.conbuildmat.2008.07.030
31. Cook G (2018) Early life flexural performance and behavior of reinforced BCSA concrete beams
32. Golaszewski J, Cygan G, Golaszewska M (2019) Development and optimization of high early strength concrete mix design. In: IOP conference series: materials science and engineering, vol. 471, Institute of Physics Publishing. https://doi.org/10.1088/1757-899X/471/11/112026
33. Mousa MI (2015) Flexural behaviour and ductility of high strength concrete (HSC) beams with tension lap splice. Alex Eng J 54:551–563. https://doi.org/10.1016/j.aej.2015.03.032
34. El-Azab A, Mohamed HM (2014) Effect of tension lap splice on the behavior of high strength concrete (HSC) beams. HBRC J 10:287–297. https://doi.org/10.1016/j.hbrcj.2014.01.002
35. El-Azab MA, Mohamed HM, Farahat A (2014) Effect of tension lap splice on the behavior of high strength self-compacted concrete beams. Alex Eng J 53:319–328. https://doi.org/10.1016/j.aej.2014.01.009
36. Najm H, Balaguru P, Asce M (2005) Rapid-hardening concrete mixes. 17:2198. https://doi.org/10.1061/ASCE0899-15612005
37. Ibrahim W, Karim O (2020) Flexural behaviour of reinforced rapid hardened concrete beams. Int J Eng Adv Technol 9:2281–2286. https://doi.org/10.35940/ijeat.C5301.029320
38. Hossain-Zada MK, Kolagar S, Fakoor M, Vahedi A, Nematzadeh M, Tabari MMR (2023) Post-heating flexural behavior of reinforced concrete beam with lap-spliced bar and feasibility of improving flexural performance by adding hybrid fibers. Structures 55:965–982. https://doi.org/10.1016/j.istruc.2023.06.082
39. Hwang H-J, Baek J-W, Kim J-Y, Kim C-S (2019) Prediction of bond performance of tension lap splices using artificial neural networks. Eng Struct 198:109535. https://doi.org/10.1016/j.engstruct.2019.109535
40. Tepfers R (1979) Cracking of concrete cover along anchored deformed reinforcing bars. Mag Concr Res 31:3–12
41. Camps B, Schmidt M, Hegger J (2023) Anchorages and laps according to the next-generation Eurocode 2: overview and comparison to current provisions. Struct Concr 24:7043–7061. https://doi.org/10.1002/suco.202300167
42. Richter BP (2012) A new perspective on the tensile strength of lap splices in reinforced concrete members
43. ACI Committee 408 (2003) ACI 408R-03 bond and development of straight reinforcing bars in tension. American Concrete Institute, pp 1–49
44. Glucksman RL (2019) Bond strength of ASTM A615 Grade 100 reinforcement for beams
45. Goksu C, Yilmaz H, Chowdhury SR, Orakcal K, Ilki A (2014) The effect of lap splice length on the cyclic lateral load behavior of RC members with low-strength concrete and plain bars. Adv Struct Eng 17:639–658. https://doi.org/10.1260/1369-4332.17.5.639
46. Micallef M, Vollum R (2017) The effect of shear and lap arrangement on reinforcement lap strength. Structures, vol. 12, Elsevier, pp 253–64

47. Wu CH, Chen MY, Chen HJ (2018) Bond behavior of tension bar at lap splice of SCC beam. Key Eng Mater 789:126–130
48. Yasin AK, Bayuaji R, Susanto TE. A review in high early strength concrete and local materials potential. In: IOP conference series: materials science and engineering, vol. 267, Institute of Physics Publishing; 2017. https://doi.org/10.1088/1757-899X/267/1/012004
49. 318 ACIC. Building Code Requirements for Structural Concrete (ACI 318–19): An ACI Standard; Commentary on Building Code Requirements for Structural Concrete (ACI 318R-19). American Concrete Institute
50. ECP Committee-203-2020 (2020) The Egyptian code for design and construction of concrete structures. Housing and Building Research Center, Giza, Egypt
51. Ferron RD, Stacey S, Carris G, Rung M (2017) Evaluation of ASTM C 494 procedures for polycarboxylate admixtures used in precast concrete elements [Project Summary]
52. Montella A, Turner S, Chiaradonna S, Aldridge D (2013) International overview of roundabout design practices and insights for improvement of the Italian standard. Can J Civ Eng 40:1215–1226
53. EN BS. 12390-2: 2009 (2009) Testing hardened concrete. Making and Curing Specimens for Strength Tests n.d.
54. Park R (1989) Evaluation of ductility of structures and structural assemblages from laboratory testing. Bull N Z Soc Earthq Eng 22:155–166
55. Rakhshanimehr M, Esfahani MR, Kianoush MR, Mohammadzadeh BA, Mousavi SR (2014) Flexural ductility of reinforced concrete beams with lap-spliced bars. Can J Civ Eng 41:594–604

Publisher's Note

Mohamed Hussein El Fakhrany is structural engineer worked at national authority of tunnels and researcher at Helwan University—Mataria Branch.

Amal el-Zamrawi is associate professor worked at Helwan University—Mataria Branch.

Wael Ibrahim is assistant professor worked at Helwan University—Mataria Branch. He had Ph.d. in Civil and environment at University of Aachen, RWTH, Germany, and M.Sc at Faculty of Engineering, Helwan University—Mataria—July 2002.

Alaa Sherif is professor worked at Helwan University—Mataria Branch. He had leading researches in concrete field over long year of his work as professor of concrete structures.